Blockchain-based Decentralized Frequency Control of Microgrids using Federated Learning Fractional-Order Recurrent Neural Network

Veerapandiyan Veerasamy, *Member, IEEE,* L. P. Mohasha Isuru Sampath, *Member, IEEE*, Shailendra Singh, *Member, IEEE*, Hung Dinh Nguyen, *Member, IEEE*, and Hoay Beng Gooi*, *Fellow, IEEE*

***Abstract*-- This paper presents a blockchain-based decentralized frequency control of an islanded microgrid (MG) using a novel federated learning fractional order recurrent neural network (FL-FORNN). A self-adaptive proportional-integral-derivative (PID) controller is proposed using FL-FORNN to handle the uncertainties of power generation by the prosumers while participating in the trading of the islanded MG. In this work, the frequency oscillations during peer-to-peer (P2P) energy trading are regulated through the appropriate design of an adaptive controller and the implementation of a smart contract participation matrix (SCPM) for balancing the generation and consumer demand. A Proof-of-Authority (PoA) private blockchain-based SCPM has been developed to secure the contract among peers. The SCPM provides the power demand information from a consumer to a prosumer who participates in the P2P energy market. It also provides power reference to the prosumer distributed generation as a supplementary control, in addition to the secondary frequency control of the system. To study this, an islanded MG comprising four source nodes (prosumers) and three demand nodes (consumers) are tested with the implementation of the PoA-based blockchain framework. With its SCPM calculation running in the blockchain framework, the decentralized control of prosumers is implemented by interfacing the OPAL-RT with Raspberry Pi devices. The robustness of the proposed FL-FORNN controller has been verified with the FORNN tuned PID controller. Furthermore, a comparative analysis is made with centralized scheme and traditional decentralized frequency control technique.**

***Index Terms*—decentralized frequency control, peer-to-peer energy market, blockchain, smart contract participation matrix, federated learning.**

I. INTRODUCTION

Recent development in cryptocurrencies and blockchain led to the digital transition of conventional unilateral power grids into peer-to-peer energy (P2P) trading with the proliferation of communication technologies, IoT (Internet of Things), and intelligent smart meters [1]. P2P energy trading is the next-generation smart grid network that enables proactive customers to participate independently in energy trading with prosumers and the grid [2], [3]. The various advantages of P2P energy trading are increasing penetration of renewable energy (RE) generation, reduced emission, electricity and investment cost, peak-load shaving, and reliable power through prosumer/consumer-based energy management [4], [5]. However, the centralized control and supervision of energy management are no longer applicable; hence, decentralized methods and structures are more extensively used for P2P energy networks. Further, the integration of a substantial number of uncertain RE sources increases the frequency oscillations of the smart grid system [6]. To mitigate this issue, a frequency regulation market has become a crucial part of ancillary service markets but faces several challenges due to increased transactions. In addition, the system operator bears significant work on fee settlement, data storage, and market information. The prosumers and consumers who participate in the trading have doubts about their transactions in some instances, and it is not easy to trace them [7]. To resolve this issue, a decentralized distributed ledger, blockchain technology, has been introduced into the energy market, inspired by its intrinsic characteristics of the data that cannot be tampered easily and have more security [8]. In this work, we attempt to use a traceable frequency regulation transaction system for an islanded microgrid (MG) with prosumers and consumers participating in trading to enhance transaction transparency and safety in energy markets.

A. Related Works

The increase in load demand has led to the development of RE-based MG operating in islanded and grid-connected modes. In islanded MGs, the control objectives are frequently determined and employed using a multi-layer hierarchical structure to set the frequency and voltage to their desired values and to produce accurate active and reactive power sharing [9]. The regulation of voltage and frequency are the prime objectives of primary control in the MG. It shares the active power among the distributed generators (DGs) based on their ratings [10]. However, the primary control can lead to slight frequency deviations from the nominal frequency. To restore the frequency to its nominal value, the secondary control called load frequency control (LFC) is applied to maintain the balance between the generation and load demand. This results in retaining the system frequency within the permissible limit of ±

This research is supported by the National Research Foundation, Singapore under its NRF-EMA EMA-EP004-EKJGC-0003 Award, EMA-ESG under its NRF2019NRF-CG002-002 Award, A*STAR under its 2nd Singapore-Germany Academic-Industry 2+2 Collaboration under Award A1990b0060, MOE ARF Tier 1 2019-T1-001-119 Award, NTU SUG 001500-00001, and Office of Naval Research Global (ONRG), USA under CODE 33D, Naval Energy Resiliency and Sustainability in Broad Agency Announcement N00014-18-S-B001, and ONRG under Award N62909-19-1-2037.
(*Corresponding Author: Hoay Beng Gooi*)
Veerapandiyan Veerasamy, Shailendra Singh, Hung Dinh Nguyen, and Hoay Beng Gooi are with the School of Electrical and Electronics Engineering, Nanyang Technological University, Singapore 639798. email: {veerapandiyan.v, shailendra.singh, hunghtd and ehbgooi}@ntu.edu.sg.
Lahanda Purage Mohasha Isuru Sampath is with the Institute of High Performance Computing (IHPC), Agency for Science, Technology and Research (A*STAR), 1 Fusionopolis Way, #16-16 Connexis, Singapore 138632, Republic of Singapore. email: mohasha_sampath@ihpc.a-star.edu.sg

0.2 Hz [11], [12]. The traditional centralized controllers were adopted for LFC study of the MG system. The centralized controllers follow the droop characteristics of the plant better but require considerable data transfer bandwidth which is less reliable and suffers from communication delay. Hence, decentralized control was typically employed as it is a communication-free control structure. Although this scheme benefits in many aspects, in general, they provide a sub-optimal solution as each DG is controlled locally by its own states. On the flipside, the tertiary control is used for economic dispatch and optimal power flow.

The traditional LFC are non-cooperative for frequency control of MGs or multi-area systems. The conventional PID controller is widely used because of its simple structure and implementation. Besides, robust control techniques like sliding mode control (SMC) [13], H-infinity [14], and model predictive controllers are used in a centralized manner to regulate the frequency of the system [15]. These conventional feedback controllers cannot guarantee the performance for a wide range of system parameter changes [16]. To ensure system stability, adaptive controllers based on machine learning (ML) were proposed for LFC applications. For example, in [17], the authors propose a learning-based SMC where the recorded data are used to optimize the parameters of the SMC controller leading to an optimal closed-loop response. The adaptive decentralized control of the multi-agent system was studied to regulate the frequency of the hybrid power system [18]. Multi-agent deep reinforcement learning is used for co-operative frequency control of interconnected systems considering the non-linearities such as generator rate constraints and governor dead band [19]. The authors in their previous work [11] use a stochastic gradient descent-based recurrent neural network (RNN) to design an adaptive PID controller to achieve the frequency regulation of the RE integrated system. However, when using the ML techniques for adaptive controller design, the local data can be insufficient to train the learning model due to the limited available memory. Further, the case of large uncertainties due to the intermittent nature of RE sources integrated into the MG network may result in substantial oscillations of system frequency. Thus, the controller trained using local data may fail to adapt to such large dynamics. Hence, an effective control design using cooperative learning of neural networks may resolve such problems.

To this end, the federated learning (FL) of the network cooperatively trains the control models based on the data available in their local memory and then a parameter server that can aggregate the trained models. This step is repeated until the controller reaches a steady-state response [20]. The FL has been exploited for autonomous vehicle control [21] and anomaly detection in industrial control systems [22]. In [23], the authors applied the FL framework with multi-agent reinforcement learning for voltage control of distribution network. Another application of energy theft detection in smart grid [24] and design of autonomous controller for connected vehicle [25] are studied. In FL, a number of nodes can store and process the data locally, and they collaboratively train the model and share the parameters with other nodes. It makes the controller converge to the optimal learning model and operate for wide range of scenarios of real-time P2P electricity market in the presence of uncertainties and environmental dynamics. Hence, we propose a FL based approach to enable privacy-preserving collaborative network model for decentralized frequency control application.

On the other hand, fractional-order calculus has a history of 300 years. It has been applied to many fields in the past few decades due to its infinite memory and heredity to integer orders [26]. Based on fractional-order (FO) calculus, the fractional order recurrent neural network (FORNN) concept has been developed as an enrichment of integer-order RNN. The FO derivative are nonlocal and have singular kernels, which give rise to more degree of freedom and infinite memory for fractional systems. Pu et. al [27], is the first one to study the mathematical formulation of dynamic associative RNN for defense against chip cloning attacks. The outcome shows that the fractional networks attractors essentially relate to the neurons FO significantly. Liu et. al. [28] addressed the synchronization of FORNN with time-varying delays under event-triggered communication to preclude Zeno behaviors. Yang et al. [29] used the fractional stochastic gradient descent approach to improve the updating method of network parameters for classification of MNIST datasets. Furthermore, the significant performance of FORNN is demonstrated for state-of-charge estimation of battery [30], decision making process of multi-underwater unmanned vehicle [31], and its stability properties is extensively investigated in [26] with linear activation function. In [32], the authors demonstrated that FORNN are the reduced-order representation of infinite entire network models with infinite memory which reduces the number of parameters and system complexity. In addition to the FO network, the FL framework enables a time-varying participation of prosumers in P2P trading by adjusting the control decision to achieve a desired frequency. To adapt the trading at different times, the frequency that FL update the control parameters will be time-varying. In other words, by solely training with local data, the controller will work in limited scenarios but not in presence of more general P2P energy trading pattern which could jeopardize the stable operation of the power system. To address this challenge, a federated learning-based FORNN (FL-FORNN) decentralized frequency control for P2P energy trading is proposed.

In deregulated energy markets like P2P energy trading, the proliferation of prosumers and consumers-based MG suffer from privacy, security, and performance bottlenecks. To achieve this, blockchain-based P2P energy trading is more necessary, as the peers can communicate with each other by invoking the energy contract [33]. Blockchain effectively secures the information exchanged among peers due to its cryptographic mechanism and verification process. Owing to these advantages, this has been proliferating in the power system domain [3].

Blockchain is a distributed ledger that records the transaction information of each nodes participate in the network [34]. The blockchain is used for decentralized energy management for scheduling of distributed energy resources in the virtual power plant [35]. The authors in [36], design a decentralized blockchain enabled voting-based consensus mechanism for P2P trading in internet-of-things-based smart grid. Their proposed blockchain records the smart meters data and provides transparency and immutability properties while trading.

According to the preceding research work several consensus protocols such as proof-of-work (PoW), proof-of-stake (PoS) and practical Byzantine fault tolerance (PBFT) are much needed in order to achieve consensus among the nodes in the blockchain network. The authors in [8] concluded that none of the blockchain models could match the sampling rate of the control system for power system application. As the control system, samples, the electrical parameters to be controlled more than 10000 times per second. This means the mining rate of blocks must be equivalent to the sampling rate and generate 10000 blocks per second. Also, the PoW and PoS need complex mining mechanism and huge gas fee [34]. Particularly, the choice of blockchain technology depends on the specific application, with either public or permissioned blockchains being viable options. Regardless of the type of blockchain used, block creation must be distributed among participants or a sufficient number of independent miners. For several reasons, Proof-of-Authority (PoA) consensus mechanism, is a good choice for energy trading applications [34, 37].

- *Efficiency gains* - PoA is faster and use less energy than alternative consensus techniques like PoW, which might be important in applications that require energy trading to be completed in a timely manner.
- *Enhanced security* - PoA is less vulnerable to malicious attacks than public blockchains because block validators are pre-selected and recognized. This is crucial in the energy trading industry since transaction integrity is essential.
- *Increased transparency* - PoA can be set up to offer a high level of transparency, which can boost confidence in the energy trading process and lower the likelihood of disputes.
- *Better scalability* - PoA is particularly suited for scalable implementation of energy trading with increased prosumer participation since it can handle more transactions per second than other consensus processes.
- *Reduced costs* - PoA does not require large amounts of computational power to validate blocks, reducing the cost of energy trading compared to other consensus mechanisms.

Motivated by this, the authors use a PoA based private blockchain to develop a smart contract for supplementary control and energy trading in the MG network. In the power market, an energy contract or smart contract is a key element that runs in the blockchain platform without a human interface. A smart contract is well suited for end-to-end energy transactions among peers to ensure the security and fairness of decentralized energy systems [8], [38]. However, the scope is limited to energy trading and has an insignificant concern about the system's operation and stability. As the penetration of RE prosumers into the open energy market increases the frequency oscillations more than the centralized system. Hence, frequency regulation is proposed for open decentralized market system.

B. Motivation and Contribution

With the increasing intelligence of power systems, technologies such as artificial intelligence, edge computing, and blockchain are widely used in industrial control system. Researchers have used the blockchain-based techniques to establish a decentralized energy trading markets and realized them transparently. These approaches can directly connect the prosumers and consumers by simplifying the multilevel structure of the existing complex power system. However, the scenarios that these approaches focus are simple and did not consider the effect of secondary frequency control. But assumed that the peers in trading should resolutely obey the dispatching plan. It is hard to efficiently ensure the frequency stability of the grid in a high penetration of RE system. Hence, we propose a blockchain-based decentralized frequency control to fully mobilize the low- carbon technology users and protect the frequency stability of high distributed energy resources (DERs) penetrated MG system.

The traditional LFC framework adopted to regulate the frequency oscillations is no longer applicable to the P2P energy trading system, since the LFC reserve is procured through energy contracts. As there are several prosumers in the P2P energy market with competitive prices. Hence, the consumers have the freedom to establish a contract with any prosumer for transaction of power with minimum bidding price. A consumer can have contract with one or more prosumer and the market need to be cleared through a double action mechanism. This makes several combinations of prosumer-consumer contracts possibilities in actual practice. Hence, we introduce the concept of “contract participation matrix (CPM)” to make the visualization of contracts. In order to secure the information against invaders in injection of false data, the concept of CPM is coded in blockchain and so-called “smart contract participation matrix (SCPM)”. Now, the information is no longer tampered and hence, a new framework for LFC is developed. This allows the consumers to go into bilateral contracts with prosumers who sell the energy at a minimum price and bid the energy based on their anticipated load requirement is implemented.

In our approach, the LFC problem is reformulated and employed for the P2P energy trading system through the concept of a SCPM development similar to Disco participation matrix in the deregulated environment as proposed in [39]. In this work, the SCPM is developed in blockchain with a set of rules coded inside the blocks which act as a supplementary control in addition to the secondary controller to maintain the frequency stability of the system. The information flow of the SCPM is superimposed on the conventional LFC system, and the results reveal some interesting patterns. Whenever a load demanded by the consumer changes, it is reflected as a local demand. This will be reflected at the point of input to the power system block. As there are many DGs in the MG, the control error will be distributed in proportion to their participation in the LFC.

Unlike the traditional LFC system, in P2P energy trading a consumer asks a particular prosumer for load power. This demand is reflected in the dynamics of the system which respond to this power command. Thus, a particular set of prosumers supposed to follow the load demanded by the consumer. Thus, the information flows from consumer to a particular prosumer specifying its demands. Here we introduce the information signals from an additional supplementary control which are absent in the traditional LFC scenario. In order secure the contract against fraudulent transactions, the blockchain technology promises in delivering optimistic use-value with transparency among all peers who participate in the transaction. To the best of the authors' knowledge, a fully decentralized frequency control of the P2P energy trading system is still unaddressed in the literature.

The main contribution of this paper are as follows:

- A PoA-based private blockchain network for P2P energy trading between prosumers and consumers is implemented through the SCPM calculation and integrated with the decentralized frequency regulation of the MG system.
- A federated learning technique is embedded with a FORNN-based PID controller design to enhance the frequency regulation of islanded MG systems.
- The implementation of the blockchain-based decentralized frequency control is demonstrated for an islanded MG system to prove the feasibility and effectiveness of the proposed control technique.
- The developed frequency control algorithm has been validated in real time through the hardware-in-the-loop testing by interfacing OPAL-RT with Raspberry Pi devices to run as the blockchain nodes.
- The performance of the proposed decentralized control scheme is benchmarked against the centralized method and traditional LFC system.

IV. A case study through the implementation of SCPM and the FL-FORNN PID controller for frequency regulation is demonstrated in addition to comparison of different control schemes in section V. Finally, the conclusion and future scope are presented in the last section of this paper.

II. Overall Framework of Decentralized Frequency Control

Fig. 1 depicts the decentralized frequency control framework of the islanded MG setup with P2P energy trading in RT-LAB operated in a real-time simulator machine. In this paper, the proposed blockchain is set up for trading between the prosumers who produce the energy and sell it to the consumers by agreeing the smart contract. The contract is developed by applying a set of rules which are discussed in the forthcoming sections. Fig. 1 has three modules for implementing the proffered decentralized LFC for the open P2P energy market. In Module-1, the P2P energy trading occurs using a double auction among the prosumers and consumers by clearing the market. The information of the amount of power shared between the prosumers and consumers in the open electricity market is developed as a *Smart Contract Participation Matrix* by accepting the trading price. The SCPM gives the power

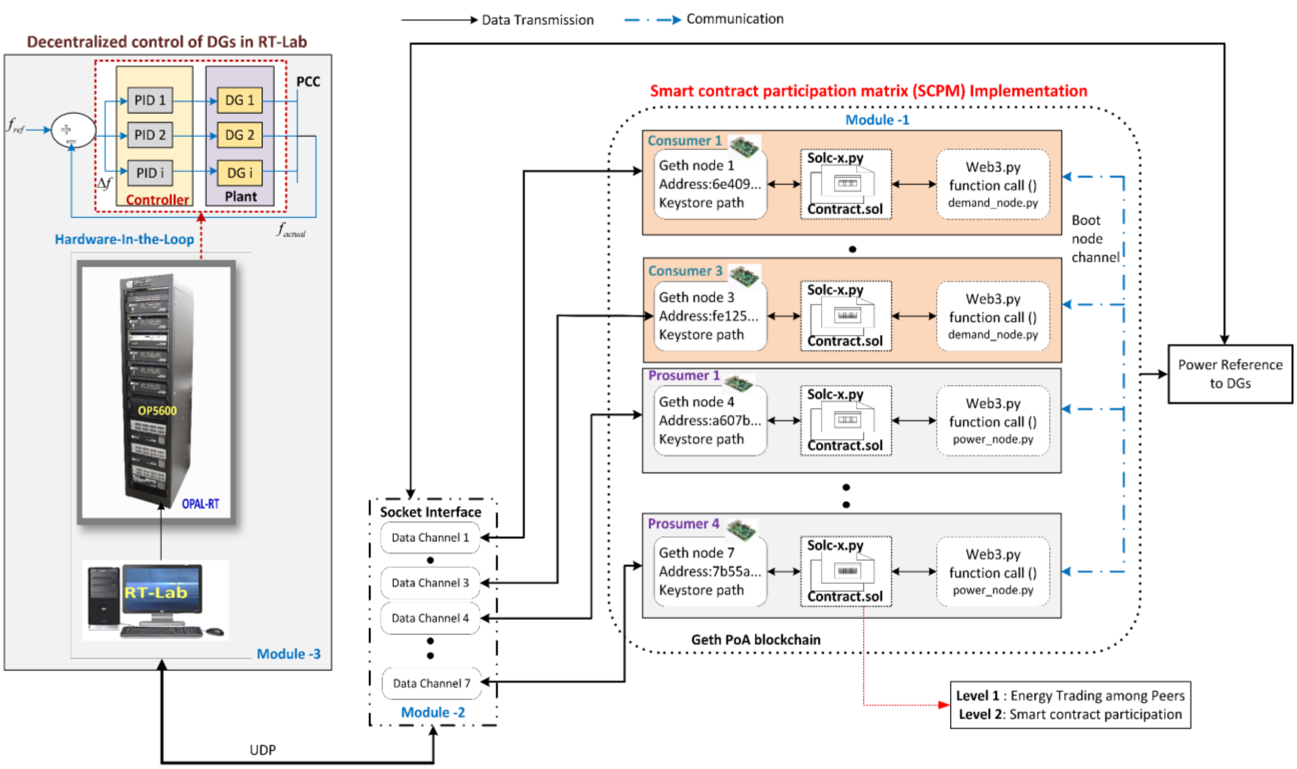

Fig. 1. Framework of blockchain-based decentralized control of MG

The remaining section of this paper is structured as follows: Section II describes the islanded MG model with the implementation of the decentralized frequency control. Section III presents the PoA private blockchain-based SCPM calculation for frequency control of the energy trading system. The design of the FORNN based PID controller with FL for decentralized control of an islanded MG is discussed in section

references to the power producers (prosumers) that act as supplementary control for regulating the frequency of the open energy market system. In addition to the traditional LFC, the proposed work has a supplementary control that helps to smoothen the frequency oscillations by giving an additional power command to the prosumers to meet the consumer demands. Module-2 is a socket interface to transfer the data at low latency through *User Datagram Protocol* (UDP) between the islanded MG model developed in RT-LAB with a private Ethereum blockchain that includes seven data transfer channels, four prosumers and three consumers. The data are packed and grouped for further transmission to the blockchain system using *Remote Procedure Calls* that provide authentication and bidirectional streaming. Then, the received power reference data are used as a supplementary control in addition to the primary and secondary control of the islanded MG in Module-3. The islanded MG model in this work considers four prosumer supplying consumers which are modelled using the linearized transfer function in MATLAB/Simulink and implemented in RT-LAB with the proposed FL-FORNN controller.

A. Decentralized control

The decentralized secondary control at each DG uses the information from its individual states and acts rapidly compared to the centralized controller. In this manner, the state of neighbor DGs in the MG is estimated based on its local measurements. The determining variables are used to generate the appropriate control action to the primary layer for regulating the plant's output to achieve a stable frequency of the MG system [6], [18]. Fig. 2 depicts the decentralized frequency control of the islanded MG system consisting of a primary droop and secondary frequency controller. The load demand of consumer ΔP_d may influence the MG frequency Δf_i, which can

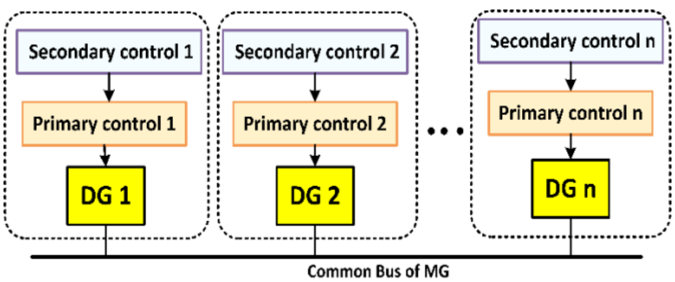

Fig. 2. Decentralized control of islanded MG

be regulated within the permissible limit of ±0.2 Hz by maintaining the generation and load balance. This is achieved by minimizing area control error (ACE) using a secondary controller. Hence, a decentralized frequency control is employed to regulate the system frequency while maintaining the proportional active power sharing among the DGs in islanded MGs.

B. System Model

This section presents the linearized model of the islanded MG system as shown in Fig. 3. This figure comprises the linearized transfer function model of a diesel engine generator (DEG), and RE sources like wind, and solar photovoltaic (SPV) with a battery energy storage (BES) system. The transfer functions of wind generation (WG) and SPV are actuated by uncertain solar irradiation and wind profiles, respectively. In this article, each DG source is assumed as a prosumer to participate in P2P energy trading initially by submitting its maximum capacity and selling price. Similarly, the consumer submits it's bidding price and maximum demand to establish trading. This work proposes a bilateral contract network as a flexible market design for P2P energy trading. A double auction pricing mechanism is employed for trading the energy between prosumer and consumer, which is explained in [5]. The proposed market design runs on the tertiary control layer, which is used to direct the energy flows on a relatively small-time scale. The lower-level control layers, such as primary and secondary control, are still required to maintain the stability of the system [1]. In other words, the lower-level control layers maintain the supply-demand balance when RE or load demand variations occur within individual trading intervals. A key market design objective is to find a flexible price that ensures prosumers and consumers reach an agreement on a set of contracts that constitute a stable power outcome. This process is described as a supplementary control for LFC application.

The MG model studied for LFC of the open P2P energy market comprising four distributed prosumers supplying three consumers' demand through trading. The maximum capacity of prosumers such as DEG, SPV, WG, and BES is 700 kW, 500 kW, 500 kW, and 300 kW, respectively, with the overall capacity of MG being 2,000 kW operating in islanded mode. The time-domain model of the islanded MG for frequency analysis is shown in Fig. 3. The system dynamics of islanded MG system can be represented by the differential equations and whose parameters are given in Appendix.

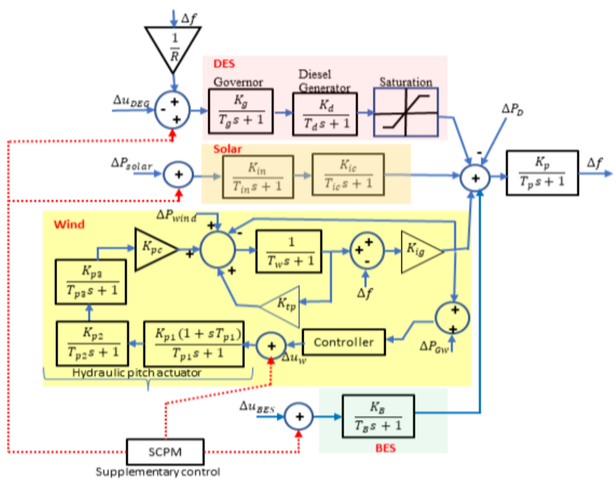

Fig. 3. Linearized model of islanded MG prosumers [40].

C. SCPM Construction

In the P2P energy trading market system, prosumers sell the energy to other consumers or prosumers or the utility grid at competitive selling prices. Thus, consumers have the liberty to choose the prosumers and establish energy contracts based on their acceptable bidding price. This allows the development of SCPM to visualize the contracts during energy trading. SCPM is a matrix with the number of rows equal to the number of prosumers selling the energy and the number of columns equal to the number of consumers demanding the energy in the network. Each entry in the SCPM represents a fraction of the total load demand contracted by a consumer (in columns) from a prosumer (in rows). The sum of all entries in each column of SCPM is always unity representing the consumer demand is fully satisfied. The SCPM illustrates, the participation of prosumer-consumer pairs in energy contracts between each other. The SCPM is constructed within the smart contract (hence named as the *Smart contract participation matrix*) and embedded in the *blocks* created in each interval of the blockchain network. These blocks form a chain over the time and the information is distributed over the nodes of the entire blockchain network. It should be noted that blockchain is an effective tool that can secure information exchange during the energy trading mechanism. In the following, the steps involved in developing the SCPM are summarized. Let the P2P energy trading framework represent m prosumers and n consumers who establish energy trading contracts.

Step-1: Initialize the elements of SCPM as zeros with the dimension of $m \times n$ representing m number of prosumers and n number of consumers.

$$\mathrm{SCPM} = \begin{bmatrix} c_{11} & c_{12} & \cdots & c_{1n} \\ c_{21} & c_{22} & \cdots & c_{2n} \\ \vdots & \vdots & \ddots & \vdots \\ c_{n1} & c_{n2} & \cdots & c_{mn} \end{bmatrix} \quad (1)$$

The element 'ij' in the matrix represents the fraction of total power contracted by the consumer j from a prosumer i.

Step-2: Receive the selling and bidding prices from both the prosumers and consumers participating in P2P energy trading, respectively. In this work, a double auction-based iterative pricing mechanism is used for market clearing, which is

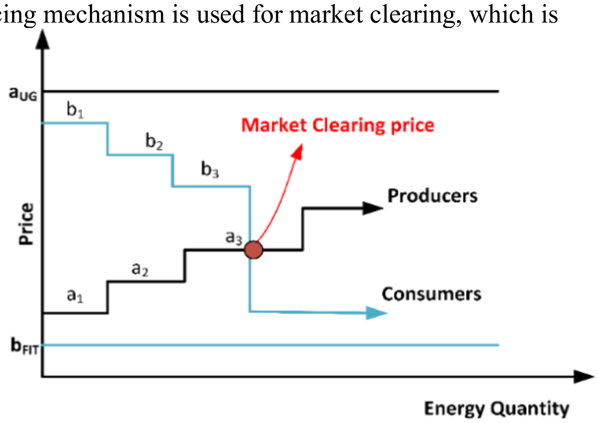

Fig. 4. Double auction pricing mechanism.

discussed in [5], [8]. In the double auction, the bidding prices of consumers, i.e., $b_1, \ldots, b_n$, are sorted in *descending order* with regard to the price offered by the utility grid (UG),

$$b_1 > b_2 > \cdots > b_n > b_{\mathrm{FIT}};\ \ n = 3 \quad (2)$$

where b_{FIT} depicts the feed-in tariff (FIT) offered by UG for prosumers. Conversely, the selling prices of prosumers, i.e., $a_1, \ldots, a_m$, are sorted in *ascending order* regarding the price offered by UG,

$$a_1 < a_2 < \cdots < a_m < a_{\mathrm{UG}};\ \ m = 4 \quad (3)$$

where a_{UG} depicts the wholesale market price from UG. Fig. 4 illustrates the market clearing mechanism of producers and consumers participating in the P2P energy market. Therein, the market clearing price will be the *mid value* of a_3 and b_3.

Step-3: Calculate each element of a column in SCPM in a way that the sum of each column of SCPM is one to meet the consumer demand at the optimal price.

Step-4: For each element, check the generation of prosumer or producer G_i is greater than or equal to the demand D_j (i.e., $G_i \geq D_j$). The element

$$c_{ij} = \frac{G_i}{D_j} \approx 1 \quad (4)$$

as the maximum value of entry is 1 which satisfies the consumer demand. Then, update all prosumers m as, $G_{i,temp} = G_i - D_j$. Set all other elements in the respective column as zero and increase the consumer count by $j = j + 1$ until n. Else if $G_i < D_j$, then calculate the element of SCPM using

$$c_{ij} = \frac{G_i}{D_j} \quad (5)$$

Then, update D_j as, $D_{j,\mathrm{temp}} = D_j - G_i$ and set $D_j = D_{j,\mathrm{temp}}$. Now, set $G_i = 0$ and increase the prosumer count by $i = i + 1$, and if $G_i \geq D_j$,

$$c_{ij} = 1 - \sum_{i=i-1} c_{ij} \quad (6)$$

Then, update G_i as, $G_{i,\mathrm{temp}} = G_i - D_j$ and set $G_i = G_{i,\mathrm{temp}}$, if $\sum c_{ij} = 1$. Increase $j = j+1$ until becomes n.

Step-5: Repeat Step-4 for all $j=1,\ldots,n$ such that all the consumer demands are satisfied.

III. PoA-based Private Blockchain

The proof-of-authority (PoA) mechanism is a fault-tolerant Byzantine consensus algorithm. The PoA consensus protocol defines the nodes that have permission to validate the transaction based on the "reputation" of nodes in the network. Therefore, running a small and private network, the PoA consensus technique was used [2], [27]. In PoA, the value of user's identification in the network is increased by using the consensus process. To verify the transactions, nodes with high "reputation" will be chosen. These nodes are preapproved as trustworthy validators and system administrators to check the transactions and protect PoA blockchains. Only the predetermined validators can process the transactions and construct the blocks. As the chain is built up by each validator in turn, the overall weight and cost are kept to a minimum value [8]. The main advantages of the PoA mechanism are less computational burden compared to the PoW mechanism, no trust issues among the participants [3], [8]. Hence, more transactions per second can be executed. Consequently, the PoA-based blockchain has been used to implement a decentralized energy marketplace, and the gas fee of transactions is set as zero specifically to facilitate trading platform development. The most crucial component of the PoA blockchain is the 'transaction ledger'. It tracks all the blocks that contain database transactions. Then, add, update, or remove the data, for example, a transaction that is saved in a block will be added to the transaction ledger. The middleware serves as a bridge between the application and the PoA blockchain. It helps to link the front-end to the database and the PoA blockchain [2], [3].

A. Implementation of SCPM in PoA Blockchain

The SCPM has been implemented in the blockchain using python scripts, and the smart contract is developed using a solidity language. The detailed steps are as follows:

Step-1: Initialize the nodes to start the blockchain

Based on the developed scripts ("startnode.cmd"), run the boot node (node-0) and then run other nodes (equal to number of prosumers (m) and consumers (n) participating in trading, respectively) to start and connect with blockchain.

Step-2: Start the timer to control the cycle loop

Create a python file ("timing.py") that controls the period of the cycle loop and does reset for each cycle so that new data for new cycle can be stored and analyzed. Besides, the summary of results will be shown in the terminal running "timing.py", which indicates the amount and price of consumer demands; maximum capacity dispatched amount and price of prosumer generations; allocation matrix; and power reference values.

Step-3: Obtain the demand data and sort the bidding price in descending order

Initially, the quantity and price for each consumer or demand are randomly generated within a predefined range. The values will be read and stored in the blockchain by calling the functions in the smart contract. Meanwhile, an exclusive flag for this node will be turned into true which indicates that the information of this node is successfully obtained. The same procedure is repeated in other demand nodes till all the consumer flags become true. Subsequently, the demands will be sorted in descending order based on the bidding price.

Step-4: Obtain the generation data and sort the selling price in ascending order

Similarly, the maximum capacity and energy price of each prosumer or producer is randomly generated and stored in the blockchain by calling the corresponding functions. Once their flags are turned as true, the data would be sorted in ascending order of selling price.

Step-5: Dispatch of generation for demand

In this scenario, the consumers will be allocated to the prosumers based on the "Power Dispatch" function, i.e., the specific allocation ratio reflected in the entries of SCPM. The steps for the implementation of SCPM are discussed in section II above. In addition, the steps for implementing SCPM in the blockchain smart contract are summarized in Algorithm 1.

Algorithm 1 Implementation of the smart contract

Start
Develop a $\boldsymbol{smartContract_i} \in [\boldsymbol{block_i}]$
Initialize each prosumer and consumer node:
$< \boldsymbol{address}[\boldsymbol{account}], \boldsymbol{uint}[\boldsymbol{id}], \boldsymbol{int}[\boldsymbol{P}, \boldsymbol{\lambda}, \boldsymbol{status}] >$
Receive data:
$< \boldsymbol{address}, \boldsymbol{id}, [\boldsymbol{P}, \boldsymbol{\lambda}, \boldsymbol{status}] >$;
Sort the prosumers and consumers based on their price;
Calculation:
SCPM calculation for $Node_1$ to $Node_{m+n}$;
Return the power reference values to prosumer nodes:
$< \boldsymbol{address}[\boldsymbol{account}], \boldsymbol{uint}[\boldsymbol{id}], \boldsymbol{int}[\boldsymbol{P}, \boldsymbol{\lambda}, \boldsymbol{status}] >$
Repeat next cycle
end

Step-6: Validation

Consider the case of four prosumers and three consumers participating in trading. In this scenario, the frequency regulation of the P2P energy trading system is studied. The allocation matrix obtained after implementing the SCPM in blockchain gives the power reference value to the prosumer, which is considered as a supplementary control reference in this study. For instance, the 48th cycles of occurrence in the blockchain is shown in Fig. 5, in which D_1 is the demand with the highest price, 700 kW for \$0.7/kWh; D_2 is 449 kW for \$0.5/kWh; and D_3 is 482 kW for \$0.4/kWh; while G_1 is the generation with the lowest price, 225 kW for \$0.2/kWh; G_2 is 456 kW for \$0.2/kWh; G_3 is 600 kW for \$0.3/kWh; and G_4 is 414 kW for \$0.5/kWh. Therefore, the demand with the highest price and the generation with the lowest price will be allocated first. The computation of elements of SCPM is explained in section II C.

Following the procedure, the consumer demand D_1 is 700 kW. Here $D_1 > G_1$, where G_1 is 225 kW, their corresponding element of SCPM using (5) as:

$$c_{11} = \frac{225}{700} \approx 0.32 \tag{7}$$

Now, using step-4, $D_{1temp} = 700 - 225 = 475$ kW. D_{1temp} is greater than prosumer 2 ($G_2 = 456$ kW). Hence, the element using (5) as:

$$c_{21} = \frac{456}{700} \approx 0.65 \tag{8}$$

Calculate, $D_{1temp} = 475 - 456 = 19$ kW that is less than prosumer 3 ($G_3 = 600$ kW). Hence, the element using (6):

$$c_{31} = 1 - 0.32 - 0.65 = 0.03 \tag{9}$$

Now, update the prosumer using step-4 as, $G_{3temp} = 600 - 19 = 581$ kW. $G_{3temp} > D_2$ (D_2= 449 kW), so $c_{32} = 1$ and the prosumer 3 is $G_{3temp} = 581 - 449 = 132$ kW. At this instance, compare G_{3temp} with D_3 equal to 482 kW. Now, $G_{3temp} < D_3$, and hence the element using (5) resulting in:

$$c_{33} = \frac{132}{482} \approx 0.27 \tag{10}$$

Now, update $D_{3temp} = 482 - 132 = 350$ kW; this value is less than G_4, and the element follows (6):

$$c_{43} = 1 - 0.27 = 0.73 \tag{11}$$

Thus, the value of SCPM are fractional values and due to limitation of solidity language. The calculations are done in integer values and then their equivalent fractional values are used for further in MATLAB simulation.

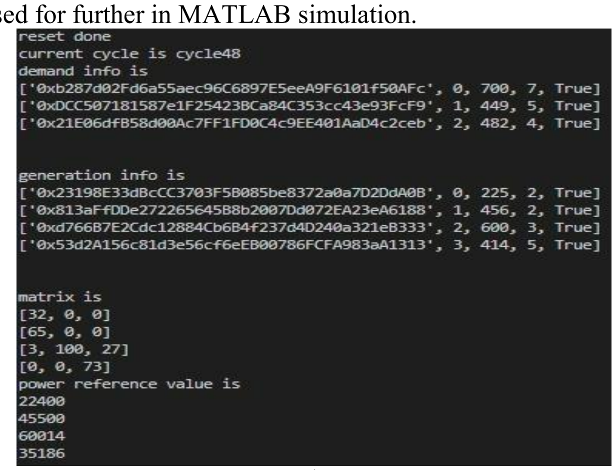

Fig. 5. Power dispatch during 48th cycle of SCPM implementation.

Therefore, the elements of the matrix and the prices are multiplied by 100 to get integer results due to the restriction of solidity language.

$$SCPM = \begin{bmatrix} 32 & 0 & 0 \\ 65 & 0 & 0 \\ 3 & 100 & 27 \\ 0 & 0 & 73 \end{bmatrix} \tag{12}$$

As a result, this power reference value represents the consumer demand satisfied by prosumers participating in the energy trading. In general, the elements of the matrices are in p.u. value of power reference and hence the maximum value of each column of SCPM will not exceed one at any instant (in case of implementation in solidity, it is 100 as given in (12)). Then, the SCPM matrix will be multiplied by the consumer demand to compute the power reference value for each prosumer as given in (13) and sent back to the plant for frequency regulation of the islanded MG model developed in OPAL-RT for analysis.

$$\begin{bmatrix} 32 & 0 & 0 \\ 65 & 0 & 0 \\ 3 & 100 & 27 \\ 0 & 0 & 73 \end{bmatrix} \times \begin{bmatrix} 700 \\ 449 \\ 482 \end{bmatrix} = \begin{bmatrix} 22400 \\ 45500 \\ 60014 \\ 35186 \end{bmatrix} \tag{13}$$

IV. Control Framework

This section presents the FORNN-based PID controller implementation for frequency regulation of islanded MG system. A detailed explanation of the network model considered is discussed in the forthcoming subsections.

A. FORNN

The implementation of RNN in real-time motivated the researchers to the development of its fractional order. About 300 years ago, the concept of fractional calculus was first presented in which the differential equations have non-integer order. In RNN, the gradient represents the dynamics of the neural network, and in the case of fractional order, this can be represented using a Caputo differential operator with respect to time as $D^{\alpha}(.)$. Equations (14) and (15) represent the dynamics of energy function (E) of FORNN [24]:

$$D^{\alpha}E = -\sum_i D^{\alpha}x_i\left[\sum_j W_{ij}f_{ij}(x_1,x_2,\ldots\ldots,x_n) - \frac{u_i}{R_i} + I_i\right], i \in n \tag{14}$$

$$D^{\alpha}E = -\sum_i C_i\, D^{\alpha}\varphi^{-1}(x_i)D^{\alpha}x_i, i \in n \tag{15}$$

where $\varphi^{-1}(x_i)$ is a monotonically increasing function and the fractional term α varies between 0 and 1. As E > 0, then the FORNN has the negative-definite fractional gradient, and the following relationship exists when the state of the neuron changes:

$$\nabla^{\alpha}E \leq 0 \tag{16}$$

where ∇^{α} is the spatial fractional derivatives of E with respect to state variables $x_1, x_2, \ldots\ldots, x_n$. In this work, the neurons $x_1, x_2, \ldots\ldots, x_n$ represent the gains K_p, K_i, and K_d of the PID controller. During the equilibrium condition, the fractional gradient becomes zero i.e:

$$\nabla^{\alpha}E = 0, \text{ if } \nabla^{\alpha}x_i = 0 \text{ for i=1,2…N} \tag{17}$$

B. Design of Self-Adaptive PID Controller using FORNN

The generalized closed loop system of FORNN-based PID controller is shown in Fig. 6 for control of plant (DG). The optimal gain parameters (K_p, K_i, and K_d) of the FORNN based PID controller are obtained by minimizing the frequency error of the interconnected system. The overall control function of PID controller is defined as follows:

$$u(t) = K_p e(t) + K_i \int e(t)dt + K_d \frac{de(t)}{dt} \tag{18}$$

where, K_p, K_i and K_d are the gain parameters of the PID controller; e(t) is the error difference between the desired value (Y_{ref}) and actual value of the plant, Y_{plant}= T(u(t)). In this work, e(t) is the ACE of the system, and for simplicity, it can be considered as:

$$e(t) = Y_{ref} - Y_{plant} \tag{19}$$

The steps to design a self-adaptive FORNN-based PID controller are detailed as follows:

Step-1: Formulation of objective Function – Define a positive value quadratic energy function using Lyapunov theorem based on the frequency error of the MG system as error signal *e(t)*. In some cases, the non-quadratic function can be chosen as discussed in [41], [42], but the robustness is studied for bounded disturbances. However, in case of P2P the disturbances are unbounded and hence the function to be minimized can be defined as (20).

$$E(K_p, K_i, K_d) = \frac{1}{2}e^2(t) \tag{20}$$

Substitute (19) in the above equation results in,

$$E(K_p, K_i, K_d) = \frac{1}{2}\left(y_{ref} - y_{plant}\right)^2 \tag{21}$$

Since,

$$Y_{plant} = T(u(t)) \tag{22}$$

On rewriting (21) using (18) and (22) results in,

$$E(K_p, K_i, K_d) = \frac{1}{2}\left\{y_{ref} - T\left[K_p e(t) + K_i \int e(t)dt + K_d \frac{de(t)}{dt}\right]\right\}^2 \tag{23}$$

Equation (23) is the objective function to be minimized for deducing the parameters of K_p, K_i, and K_d of FORNN with a linear activation function. In FORNN, the parameters are determined by computing the dynamics of the network to minimize the energy function.

Step-2: *Dynamics of Network* [11], [23] - The dynamical equations describing the gradient behavior of FORNN based on the Caputo fractional derivatives are as follows:

$$D^{\alpha}K_p = e(t)D^{\alpha}T[u(t)]e(t) \tag{24}$$

$$D^{\alpha}K_i = e(t)D^{\alpha}T[u(t)]D^{-1}e(t) \tag{25}$$

$$D^{\alpha}K_d = e(t)D^{\alpha}T[u(t)]De(t) \tag{26}$$

where, $D = \frac{d}{dt}$ is a differential operator; and ‘α’ is the fractional order term whose value ranges from 0 to 1. Equations (24) to (26) represent the RNN-based PID when ‘α = 1’ and FORNN-

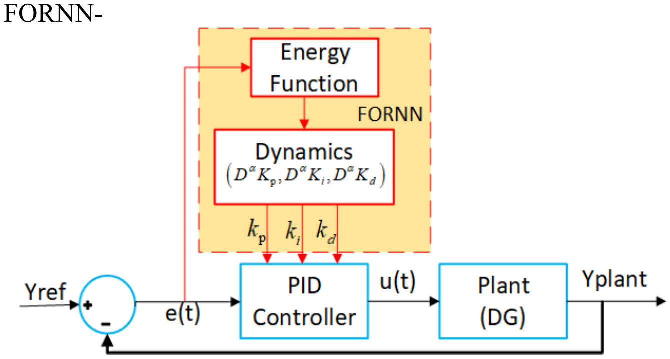

Fig. 6. Closed loop control system.

based PID controller when ‘0 < α < 1’. The fractal gradient of the energy function for updating the weight of neurons is defined as:

$$\nabla^{\alpha}E = \left[\frac{\partial^{\alpha}E}{\partial K_p^{\alpha}} \quad \frac{\partial^{\alpha}E}{\partial K_i^{\alpha}} \quad \frac{\partial^{\alpha}E}{\partial K_d^{\alpha}}\right]^T \tag{27}$$

The updating weight of the neuron using the gradients (stochastic gradient descent (SGD)) from local training data is:

$$W_{t+1,k} = W_{t,k} - \mu \nabla^{\alpha} E_{t,k}(W_{t,k}) \qquad (28)$$

Step-3: *Activation Function* **-**The gradient is used as input to the activation function of the output layer of FORNN. Thus, $K_p = \varphi(u_1)$; $K_i = \varphi(u_2)$; $K_d = \varphi(u_3)$; x_p, x_i and x_d depict the inputs of neurons, and u_1, u_2 and u_3 are the dynamics of neurons K_p, K_i and K_d, respectively. φ represents the purelin based linear activation function of output neuron and is defined as $\varphi(\cdot): \mathcal{R} \rightarrow [0 \;\; 1]$.

C. Federated Learning based FORNN

Federated learning or federated optimization is a recently emerged technique to train the ML network in a distributed way. The goal of FL is to train a NN using shared global data from a federation of participating neurons acting as a local learner under the coordination of a central server for model aggregation. The network is generally learned using a local gradient via back-propagation, as depicted in equation (28). In this research work, a centralized consensus-based FL is used. Its execution steps are detailed as pseudo-code in Algorithm 2. Further, the executing process is explained in Fig. 7. After initialization of the network, the weight $W_{0,k}$ at time t = 0, the k^{th} neuron sends its updated weight $W_{t,k}$ and receives the weights from its neighbor say i^{th} and j^{th} neuron depicted as process step-1 to 4 in Fig. 7. Based on the received information, the neuron updates its weight $W_{t,k}$ sequentially to obtain the aggregated model as [43]:

$$\psi_{t,k} = W_{t,k} + \epsilon_t \textstyle\sum_{i \epsilon N_k} \alpha_{k,i}(W_{t,i} - W_{t,k}) \qquad (29)$$

$$W_{t+1,k} = \psi_{t,k} - \mu \nabla^{\alpha} E_{t,k}(\psi_{t,k}) \qquad (30)$$

where ϵ_t is the consensus step size and can be chosen as (0, Δ), where $\Delta = max_k\left(\sum_{i \epsilon N_k} \alpha_{k,i}\right)$, the maximum degree of the graph [43] depicting the network's interaction topology. In addition to the consensus step size, the SGD step size μ is defined in such a way that the fractal gradient $\nabla^{\alpha} E_{t,k}$ decreasing with respect to time. The sharing of the weight information among neurons, calculation of aggregated model, and updating its weight and sending to other neighbors in the network are shown for the case of k^{th} neuron in Fig. 7.

Algorithm 2 Consensus-based FL-FORNN
Start procedure CFA $(\boldsymbol{N_k}, \boldsymbol{\epsilon_t}, \boldsymbol{\alpha_{t,i}})$
Initialize $\boldsymbol{W_{0,k}}$ for k^{th} neuron
for each round of t = 1, 2, … do
receive $\boldsymbol{W_{t,i}}$ from neighbors $\boldsymbol{N_k}$
$\boldsymbol{\psi_{t,k}} \leftarrow \boldsymbol{W_{t,k}}$
for all neurons $\boldsymbol{i \epsilon N_k}$ do
$\boldsymbol{\psi_{t,k}} \leftarrow \boldsymbol{W_{t,k}} + \boldsymbol{\epsilon_t \alpha_{t,i}}(\boldsymbol{W_{t,i}} - \boldsymbol{W_{t,k}})$
end for
update the weight of neuron $\boldsymbol{W_{t+1,k}} \leftarrow \boldsymbol{\psi_{t,k}}$
send $\boldsymbol{W_{t+1,k}}$ to neighbors
end for
end procedure

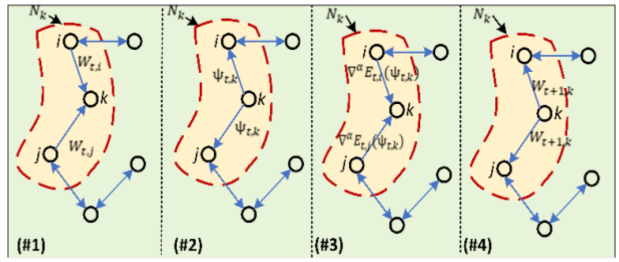

Fig. 7. Consensus-based FL-FORNN.

V SIMULATION AND RESULTS

The real-time implementation of proposed blockchain based decentralized frequency control set-up is shown in Fig. 8. The information of both the software and hardware details for the implementation of private blockchain-based frequency control are as follows: Geth (version: 1.10.6) with Node.js (6.14.6), Web3 (5.12.0.py), Solidity smart contract (>=0.4.22 and <0.7.0), Raspberry Pi (RPi) (4 Model B), RT-LAB (11.3.1.34) and MATLAB (R2021a). The MG model consider for the study consists of four prosumers and three consumers participating in P2P energy trading. The smart contract developed for energy trading and calculation of SCPM for frequency regulation of open energy market system are implemented through Raspberry Pi (RPi). The various DG prosumers participating in trading are modelled in MATLAB using a linearized model and implemented in OPAL-RT. A primary droop and secondary controller are implemented in OPAL-RT, whereas the supplementary control of SCPM calculation is implemented in RPi which gives the power reference to each prosumer after clearing the market. An UDP communication is made between the RPis and OPAL-RT model to simulate the blockchain based decentralized frequency control. The results obtained from the set-up are discussed as follows:

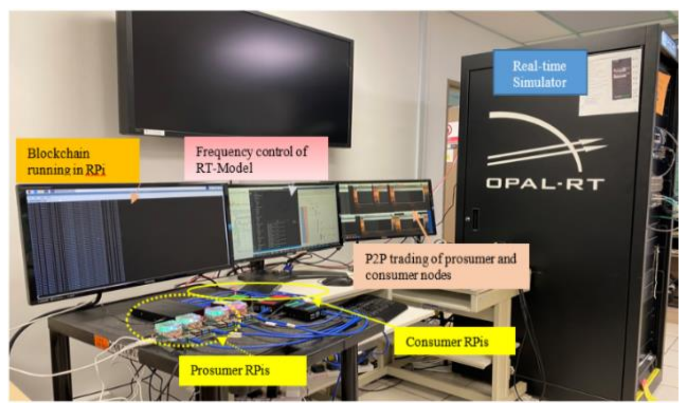

Fig. 8. Experimental setup of decentralized control of P2P energy trading system

A. Blockchain-based Frequency Control

In this scenario, the energy trading between prosumers and consumers occurs by generating a random selling and bidding price and their energy capacity. For trading to occur, the price value of each prosumer and consumer varies from \$0.20/kWh to \$1/kWh. The consumer load varies from minimum to maximum values of 350 kW to 500 kW, 400 to 550 kW, and 550 to 700 kW for consumers-1 to 3, respectively. The prosumer generation also varies between 600 to 700 kW, 400 to 500 kW, 400 to 500 kW, and 200 to 300 kW for prosumers-1 to 4, respectively, to meet the varying consumer demands. During this case of blockchain implementation, each consumer and prosumer node are implemented using RPis, and trading occurs inside the blockchain. The number of blocks generated during the mining of each authority node is given in Fig. 9. Fig. 10 depicts the bidding price and demand requirement of various consumers-1 to 3. Fig. 11 shows the selling price and maximum power dispatching capacity of prosumers-1 to 4. To start trading, the prosumers agree on the contract and compute the SCPM to meet the demand of each consumer.

The power amounts traded by the prosumers are recorded as given in Fig. 12 to meet the consumer demand shown in Fig. 10. During this case, the frequency of the MG system fluctuates when P2P trading occurs. The frequency is regulated by the implementation of supplementary control in addition to the secondary frequency controller. The supplementary control sends the power reference value after computing the SCPM in the blockchain and the secondary control gives the power command equivalent to the area control error. Both the power commands and the primary droop control regulate the P2P trading system frequency within the permissible limits of ±0.2 Hz. In this case, the system was tested with the FORNN and FL-FORNN tuned self-adaptive PID controllers, and the frequency response is shown in Fig. 13. It is clearly seen that

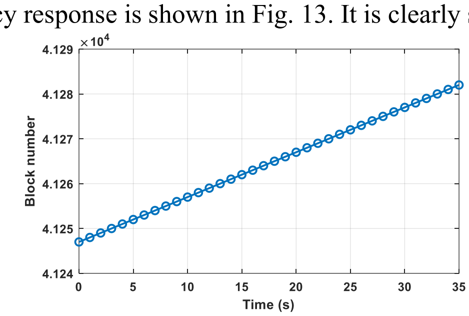

Fig. 9. Mining rate of authority nodes.

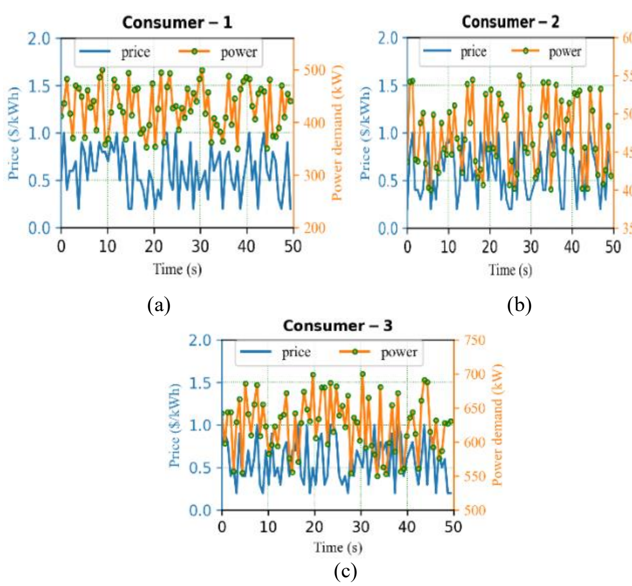

Fig. 10. Consumers bids and Power demand (a) Consumer-1 (b) Consumer-2 (c) Consumer-3 of MG participate in P2P trading.

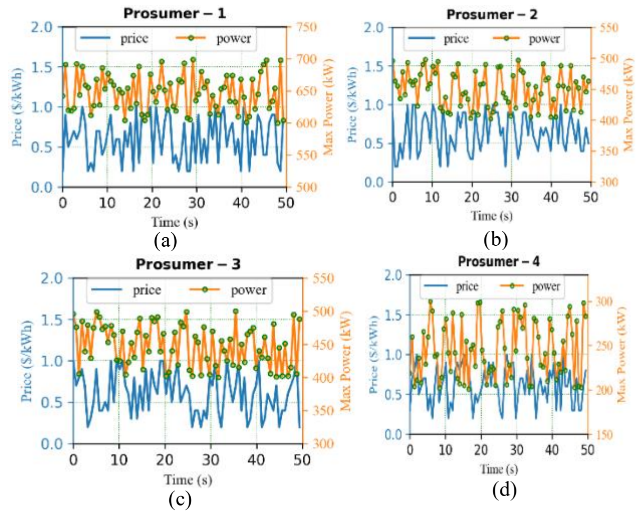

Fig. 11. Prosumers' selling price and maximum power capacity (a) Prosumer-1 (b) Prosumer-2 (c) Prosumer-3 (d) Prosumer-4 of MG participate in P2P energy trading.

the frequency oscillations are well regulated with FL-FORNN control compared to those of the FORNN method. Overall, the supplementary control with SCPM implementation in blockchain and the FL approach of the neural network effectively regulates the system frequency. Further, no prosumers or consumers can violate the contract as the contract is made through blockchain, which increases the security and satisfaction of peers who participate in the trading.

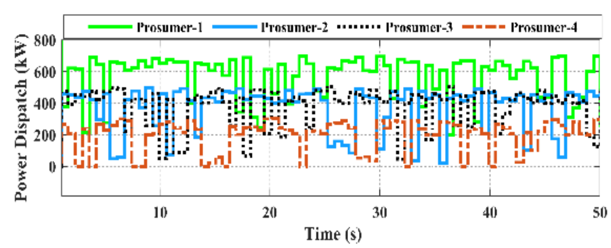

Fig. 12. Power dispatch by prosumers.

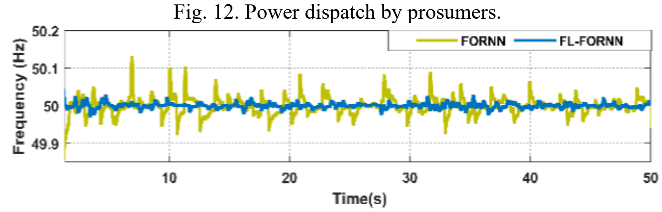

Fig. 13. Blockchain-based frequency response of islanded MG system.

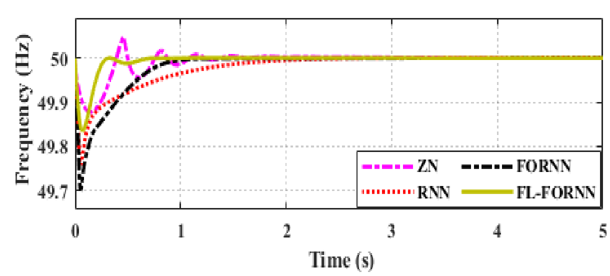

Fig. 14. Frequency response of islanded MG.

B. Comparative study

In this scenario to study the performance of the proposed controller with other state-of-the art, the various prosumers are assumed to generate constant power with fixed prices to meet the consumer demand. The prosumers-1 to 4 selling prices of \$0.5, \$0.6, \$0.7, and \$0.9 per kWh, respectively and their dispatching power: 700 kW, 500 kW, 500 kW, and 50 kW to meet the consumer demands. Consumers-1 to 3 have the bidding price of \$0.3, \$0.2, and \$0.1 per kWh, and their demand capacity of 500 kW, 550 kW and 700 kW, respectively. During this case of P2P energy trading, the SCPM was obtained to give the power reference for DG as given in (30).

$$SCPM = \begin{bmatrix} 100 & 36 & 0 \\ 0 & 64 & 21 \\ 0 & 0 & 71 \\ 0 & 0 & 8 \end{bmatrix} \tag{30}$$

It is seen that the prosumer-1 meets the consumer-1 demand fully due to its low selling price compared to that of other prosumers. The excess power of 200 kW was supplied to consumer-2, and then the remaining demand of 350 kW of power was contracted from prosumer-2 by consumer-2. Similarly, the total demand of consumer-3 was provided by prosumer-2 to 4 based on their priority of selling price. The element of SCPM shows the per unit value of power with its base value of 2,000 kW (MG maximum capacity). This power reference, in addition to the secondary controller, is supplied to the prosumer DGs to regulate the frequency of the system during P2P energy trading. In this case, the developed islanded MG model in RT-LAB is tested with well-established controllers like Zeigler Nicholas (ZN), RNN [11], and the proposed FORNN and FL-FORNN tuned secondary PID controller for validating their performance. The dynamic change in the frequency response is recorded as shown in Fig. 14. It is seen from the frequency response that the proposed FL-FORNN approach settles faster to the steady state (50 Hz) at 0.64 s, FORNN at 0.97 s, the RNN and ZN technique at 2.1 s and 2.5 s, respectively as depicted in Table 1. Almost at 2.5 s all the control techniques makes the system/plant to reach the steady state (i.e. the system frequency as 50 Hz). Since, the proposed study is a dynamic analysis of the MG system which more focus on the behavior of the system during dynamic or transient state when subjected to disturbances. In other words, the time taken to reach the steady state (i.e. settling time) is more concern during the dynamic study. From the Fig.13, it is be seen that the proposed FL-FORNN based PID controller reaches the steady state faster compared to other techniques presented. The various transient state indices measured are illustrated in Table 1. Furthermore, the computational burden can be measured based on the convergence of *Lyapunov*-based energy function defined in (20) which is illustrated in Fig. 15. Thus, the energy profile reaches the global minima by minimizing the dynamics of the network to the stable equilibrium state faster by the proposed FL-FORNN technique with minimum computational time of 0.24 s than FORNN (0.81 s) and RNN (0.99 s) approaches.

TABLE 1: TRANSIENT PERFORMANCE OF FREQUENCY RESPONSE

Control Method	Settling Time (s)	|Peak-Undershoot|	|Peak-Overshoot|	Rise Time (s)
FL-FORNN	0.6445	0.1658	0.0007	0.0067
FORNN	0.9791	0.2999	0	2.8052
RNN	2.1482	0.2417	0	1.046
ZN	2.5039	0.1222	0.034	0.0005

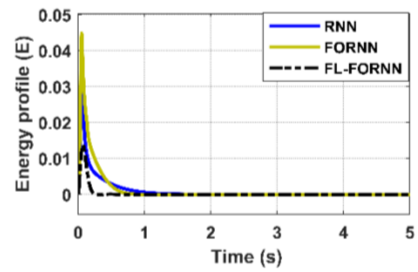

Fig. 15. Energy profile convergence of proposed network

C. *Comparative Analysis of Control Schemes*

A comparative study of proposed FL-FORNN based PID control both in decentralized and centralized mode considering the supplementary controller is discussed, in addition with the traditional decentralized control without the supplementary control. The performance analysis is made with the overall consumers loading of 75% of plant capacity. The frequency response obtained during this case is shown in Fig. 16. It is seen that the proposed decentralized scheme with supplementary control approaches the steady state frequency of 50 Hz faster compared to other techniques presented. Although the undershoot is a bit higher than the centralized control scheme, the settling time is faster. Thus, it is understood that a desirable frequency response is obtained using a sub-optimal decentralized control than the centralized approach. To validate the claim further, a study is made in the presence of RE power variation in the MG system considered. The random model for change in solar and wind power are given in [44], and their corresponding frequency response obtained is illustrated in Fig. 17. The result shows that the initial transients are high in case of centralized scheme than the decentralized approach by the proposed FL-FORNN based PID control. However, both the schemes regulate the system frequency within the standard of ±0.2 Hz with better performance being observed in decentralized method.

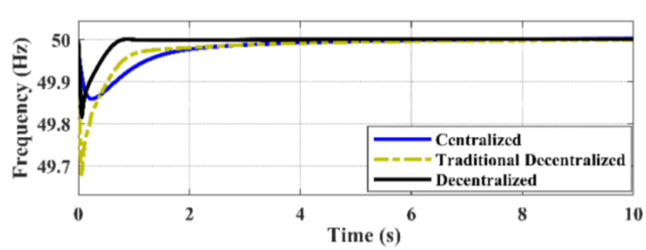

Fig. 16. Comparison of different control schemes

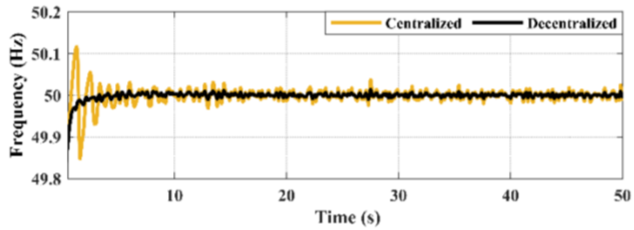

Fig. 17. Frequency response for RE power variation in MG

VI Conclusion

This paper presents the decentralized frequency control of the open P2P energy market through the smart contract implementation among the peers participating in the energy trading. A concept of SCPM has been developed and implemented in a PoA private blockchain to obtain the power reference value for prosumers to trade their energy to the respective consumers. Further, a federated learning-based FORNN designed adaptive PID controller has been developed to regulate the frequency of the open market systems within the permissible limit of ± 0.2 Hz. The robustness of the proposed FL-FORNN controller is verified against FORNN with blockchain implementation in a hardware-in-the-loop simulation set up with energy trading and SCPM computation in the blockchain. The results show that the proposed FL-FORNN approach regulates the frequency with minimum steady-state error than the centralized scheme and traditional LFC system. The study of the advanced learning of neural network for frequency regulation of the multi-microgrid system considering economic scheduling of DGs will be the future scope of this research.

Appendix

DEG: Governor gain and time constant, $K_g = 1, T_g = 0.1\ s$, Generator gain and time constant, $K_d = 1, T_d = 1.2\ s$. **Solar**: Inverter gain and time constant, $K_{in} = 1, T_{in} = 0.04\ s$, Coupling delay constant, $K_{ic} = 1, T_{ic} = \ s$. **Wind**: Hydraulic pitch actuator gain and time constants, $K_{p1} = 1.25, T_{p1} = 0.6\ s, K_{p2} = 1, T_{p2} = 0.041$. Turbine gain and time constant, $K_{p3} = 1.4, T_{p3} = 1s$. Coupling coefficient, $K_{pc} = 0.08$, Fluid coupling coefficient $K_{ig} = 1.494$. Inertia time and gain constant, $T_w = 4\ s, K_{tp} = 0.004$. **BES**: Battery gain and time constant, $K_B = 1, T_B = 0.1\ s$. Power System gain and time constant, $K_p = 100$, and $T_p = 20\ s$.

References

[1] T. Morstyn, A. Teytelboym and M. D. Mcculloch, "Bilateral Contract Networks for Peer-t-Peer Energy Trading," in *IEEE Trans. Smart Grid*, vol. 10, no. 2, pp. 2026-2035, March 2019, doi: 10.1109/TSG.2017.2786668.

[2] S. Karumba, V. Dedeoglu, A. Dorri, R. Jurdak, and S. S. Kanhere, "Utilizing Blockchain as a Citizen-Utility for Future Smart Grids," in *Wireless Blockchain: Principles, Technologies and Applications, IEEE*, 2022, pp.201-224, doi: 10.1002/9781119790839.ch9.

[3] J. Yang, J. Dai, H. B. Gooi, H. D. Nguyen and P. Wang, "Hierarchical Blockchain Design for Distributed Control and Energy Trading Within Microgrids," in *IEEE Trans. Smart Grid,* vol. 13, no. 4, pp. 3133-3144, July 2022, doi: 10.1109/TSG.2022.3153693.

[4] Tushar, W., Saha, T.K., Yuen, C., Morstyn, T., Poor, H.V. and Bean, R. "Grid influenced peer-to-peer energy trading" in *IEEE Trans. Smart Grid*, vol. 11, no. 2, pp. 1407-1418, March 2020, doi: 10.1109/TSG.2019.2937981.

[5] L. P. M. I. Sampath, A. Paudel, H. D. Nguyen, E. Y. S. Foo and H. B. Gooi, "Peer-to-Peer Energy Trading Enabled Optimal Decentralized Operation of Smart Distribution Grids," in *IEEE Trans. Smart Grid,* vol. 13, no. 1, pp. 654-666, Jan. 2022, doi: 10.1109/TSG.2021.3110889.

[6] Q. Wang et al., "A Multiblockchain-Oriented Decentralized Market Framework for Frequency Regulation Service," in *IEEE Trans. Ind. Informat.,* vol. 17, no. 12, pp. 8219-8229, Dec. 2021, doi: 10.1109/TII.2021.3062623.

[7] Q. Zhou, M. Shahidehpour, A. Alabdulwahab and A. Abusorrah, "Privacy-Preserving Distributed Control Strategy for Optimal Economic Operation in Islanded Reconfigurable Microgrids," in *IEEE Trans. Power Syst.,* vol. 35, no. 5, pp. 3847-3856, Sept. 2020, doi: 10.1109/TPWRS.2020.2985995.

[8] J. Yang, J. Dai, H. B. Gooi, H. Nguyen and A. Paudel, "A Proof-of-Authority Blockchain Based Distributed Control System for Islanded Microgrids," in *IEEE Trans. Ind. Informat.,* doi: 10.1109/TII.2022.3142755.

[9] Y. Khayat et al., "Decentralized Optimal Frequency Control in Autonomous Microgrids," in *IEEE Trans. Power Syst.,* vol. 34, no. 3, pp. 2345-2353, May 2019, doi: 10.1109/TPWRS.2018.2889671.

[10] M. Gheisarnejad, H. Mohammadi-Moghadam, J. Boudjadar and M. H. Khooban, "Active Power Sharing and Frequency Recovery Control in an Islanded Microgrid with Nonlinear Load and Nondispatchable DG," in *IEEE Systems J.,* vol. 14, no. 1, pp. 1058-1068, March 2020, doi: 10.1109/JSYST.2019.2927112.

[11] V. Veerasamy, N. I. A Wahab, R. Ramachandran, M. L. Othman, H. Hizam, J. S. Kumar, et. al., "Design of single-and multi-loop self-adaptive PID controller using heuristic based recurrent neural network for ALFC of hybrid power system" in *Expert Syst. Appl.,* vol. 192, Apr 2022, Art. no. 116402 doi:10.1016/j.eswa.2021.116402.

[12] A. Ghafouri, J. Milimonfared and G. B. Gharehpetian, "Coordinated Control of Distributed Energy Resources and Conventional Power Plants for Frequency Control of Power Systems," in *IEEE Trans. Smart Grid,* vol. 6, no. 1, pp. 104-114, Jan. 2015, doi: 10.1109/TSG.2014.2336793.

[13] D. Deepika, S. Kaur and S. Narayan, 2019 "Centralized sliding mode frequency regulation approach for an uncertain islanded micro grid integrated with disturbance observer", in *Asian J. Control,* vol. 21, no. 4, pp.2038-2048, Jan 2019, doi: 10.1002/asjc.1993.

[14] H. Bevrani, M. R. Feizi and S. Ataee, "Robust Frequency Control in an Islanded Microgrid: H∞ and μ -Synthesis Approaches," in *IEEE Trans. Smart Grid,* vol. 7, no. 2, pp. 706-717, March 2016, doi: 10.1109/TSG.2015.2446984.

[15] V. P. Singh, N. Kishor and P. Samuel, "Distributed Multi-Agent System-Based Load Frequency Control for Multi-Area Power System in Smart Grid," in *IEEE Trans. Ind. Electron.,* vol. 64, no. 6, pp. 5151-5160, June 2017, doi: 10.1109/TIE.2017.2668983.

[16] Y. Weng and H. D. Nguyen, "A New Generation of AGC using Repetitive Learning," 2020 IEEE Power & Energy Society Innovative Smart Grid Technologies Conference (ISGT), 2020, pp. 1-5, doi: 10.1109/ISGT45199.2020.9087645.

[17] D. Qian and G. Fan, "Neural-Network-Based Terminal Sliding Mode Control for Frequency Stabilization of Renewable Power Systems," in *IEEE/CAA J. Autom. Sin.,* vol. 5, no. 3, pp. 706-717, May 2018, doi: 10.1109/JAS.2018.7511078.

[18] A. Akbarimajd, M. Olyaee, B. Sobhani and H. Shayeghi, "Nonlinear Multi-Agent Optimal Load Frequency Control Based on Feedback Linearization of Wind Turbines," in *IEEE Trans. Sustain. Energy,* vol. 10, no. 1, pp. 66-74, Jan. 2019, doi: 10.1109/TSTE.2018.2823062.

[19] Z. Yan and Y. Xu, "A Multi-Agent Deep Reinforcement Learning Method for Cooperative Load Frequency Control of a Multi-Area Power System," in *IEEE Trans. Power Syst.,* vol. 35, no. 6, pp. 4599-4608, Nov. 2020, doi: 10.1109/TPWRS.2020.2999890.

[20] T. Zeng, O. Semiari, M. Chen, W. Saad and M. Bennis, "Federated Learning for Collaborative Controller Design of Connected and

Autonomous Vehicles," 2021 60th *IEEE Conference on Decision and Control (CDC),* 2021, pp. 5033-5038, doi: 10.1109/CDC45484.2021.9683257.

[21] S. R. Pokhrel and J. Choi, "Federated Learning with Blockchain for Autonomous Vehicles: Analysis and Design Challenges," in *IEEE Trans. Commun.,* vol. 68, no. 8, pp. 4734-4746, Aug. 2020, doi: 10.1109/TCOMM.2020.2990686.

[22] H. T. Truong, B. P. Ta, Q. A. Le, D. M. Nguyen, C. T. Le, H. X. Nguyen, et. al., "Light-weight federated learning-based anomaly detection for time-series data in industrial control systems" in *Comput. Ind.,* vol. 140, Sep 2022, Art. no.103692.

[23] H. Liu and W. Wu, "Federated Reinforcement Learning for Decentralized Voltage Control in Distribution Networks," in *IEEE Trans. Smart Grid*, vol. 13, no. 5, pp. 3840-3843, Sept. 2022, doi: 10.1109/TSG.2022.3169361.

[24] M. Wen, R. Xie, K. Lu, L. Wang and K. Zhang, "FedDetect: A Novel Privacy-Preserving Federated Learning Framework for Energy Theft Detection in Smart Grid," in *IEEE Internet Things J*, vol. 9, no. 8, pp. 6069-6080, 15 April15, 2022, doi: 10.1109/JIOT.2021.3110784

[25] T. Zeng, O. Semiari, M. Chen, W. Saad and M. Bennis, "Federated Learning on the Road Autonomous Controller Design for Connected and Autonomous Vehicles," in *IEEE Trans. Wirel. Commun.,* vol. 21, no. 12, pp. 10407-10423, Dec. 2022, doi: 10.1109/TWC.2022.3183996

[26] P. Liu, Z. Zeng and J. Wang, "Multiple Mittag–Leffler Stability of Fractional-Order Recurrent Neural Networks," in *IEEE Trans. Syst. Man Cybern. Syst.*, vol. 47, no. 8, pp. 2279-2288, Aug. 2017, doi: 10.1109/TSMC.2017.2651059

[27] Y. Pu, Z. Yi and J. Zhou, "Fractional Hopfield Neural Networks: Fractional Dynamic Associative Recurrent Neural Networks," in *IEEE Trans. Neural Netw. Learn. Syst.*, vol. 28, no. 10, pp. 2319-2333, Oct. 2017, doi: 10.1109/TNNLS.2016.2582512.

[28] P. Liu, J. Wang and Z. Zeng, "Event-Triggered Synchronization of Multiple Fractional-Order Recurrent Neural Networks with Time-Varying Delays," in *IEEE Trans. Neural Netw. Learn. Syst.,* doi: 10.1109/TNNLS.2021.3116382.

[29] H. Yang, R. Fan, J. Chen and M. Xu, "Recurrent Neural Networks with Fractional Order Gradient Method," 2022 14th *International Conference on Advanced Computational Intelligence (ICACI)*, Wuhan, China, 2022, pp. 49-55, doi: 10.1109/ICACI55529.2022.9837518.

[30] Y. Wang, X. Han, D. Guo, L. Lu, Y. Chen and M. Ouyang, "Physics-Informed Recurrent Neural Network with Fractional-Order Gradients for State-of-Charge Estimation of Lithium-Ion Battery," in *IEEE J Radio Freq. Identif.*, vol. 6, pp. 968-971, 2022, doi: 10.1109/JRFID.2022.3211841

[31] L. Liu, S. Zhang, L. Zhang, G. Pan and J. Yu, "Multi-UUV Maneuvering Counter-Game for Dynamic Target Scenario Based on Fractional-Order Recurrent Neural Network," in *IEEE Trans. Cybern.,* doi: 10.1109/TCYB.2022.3225106.

[32] C. Z. Aguilar, J. F. Gómez-Aguilar, V. M. Alvarado-Martínez, and H. M. Romero-Ugalde, "Fractional order neural networks for system identification, " *Chaos, Solitons Fractals*, vol. 130, 2020, Art. no. 109444.

[33] N. R. Pradhan, A. P. Singh, N. Kumar, M. M. Hassan and D. S. Roy, "A Flexible Permission Ascription (FPA)-Based Blockchain Framework for Peer-to-Peer Energy Trading with Performance Evaluation," in *IEEE Trans. Ind. Informat.,* vol. 18, no. 4, pp. 2465-2475, April 2022, doi: 10.1109/TII.2021.3096832.

[34] M. Shahidehpour, M. Yan, P. Shikhar, S. Bahramirad, and A. Paaso, "Blockchain for peer-to-peer transactive energy trading in networked microgrids: Providing an effective and decentralized strategy," in *IEEE Electrific. Mag.,* vol. 8, pp. 80-90, 2020.

[35] Q. Yang, H. Wang, T. Wang, S. Zhang, X. Wu, and H. Wang, "Blockchain-based decentralized energy management platform for residential distributed energy resources in a virtual power plant, " in *Appl. Energy*, vol. 294, 2021, Art. no.117026.

[36] J. Li et al., "Decentralized On-Demand Energy Supply for Blockchain in Internet of Things: A Microgrids Approach," in *IEEE Trans. Comput. Soc.,* vol. 6, no. 6, pp. 1395-1406, Dec. 2019, doi: 10.1109/TCSS.2019.2917335.

[37] F. Funk and J. Franke, "Matching in decentralized two-sided markets via Blockchain-based deferred acceptance," 2021 3rd *Conference on Blockchain Research & Applications for Innovative Networks and Services (BRAINS)*, Paris, France, 2021, pp. 89-92, doi: 10.1109/BRAINS52497.2021.9569823.

[38] D. Han, C. Zhang, J. Ping and Z. Yan, "Smart contract architecture for decentralized energy trading and management based on blockchains" in *Energy*, vol. 199, May 2020, Art. no.117417.

[39] V. Donde, M. A. Pai and I. A. Hiskens, "Simulation and optimization in an AGC system after deregulation," in *IEEE Trans. Power Syst.,* vol. 16, no. 3, pp. 481-489, Aug. 2001, doi: 10.1109/59.932285.

[40] M. H. Khooban, T. Niknam, M. Shasadeghi, T. Dragicevic and F. Blaabjerg, "Load Frequency Control in Microgrids Based on a Stochastic Noninteger Controller," in *IEEE Trans. Sustain. Energy*, vol. 9, no. 2, pp. 853-861, April 2018, doi: 10.1109/TSTE.2017.2763607.

[41] S. Savazzi, M. Nicoli and V. Rampa, "Federated Learning with Cooperating Devices: A Consensus Approach for Massive IoT Networks," in *IEEE Internet Things J.,* vol. 7, no. 5, pp. 4641-4654, May 2020, doi: 10.1109/JIOT.2020.2964162.

[42] M. Hosseinzadeh, and M. J. Yazdanpanah, "Performance enhanced model reference adaptive control through switching non-quadratic Lyapunov functions," in *Syst. Control Lett*., vol. 76, pp. 47-55, 2015.

[43] G. Tao, "Model reference adaptive control with L 1+ α tracking, " in *Int. J. Control*, vol. 64, pp. 859-870, 1996.

[44] A. X. R. Irudayaraj, N. I. A. Wahab, M. G. Umamaheswari, M. A. M. Radzi, N. B. Sulaiman, V. Veerasamy, et al., "A Matignon's Theorem Based Stability Analysis of Hybrid Power System for Automatic Load Frequency Control Using Atom Search Optimized FOPID Controller," in *IEEE Access*, vol. 8, pp. 168751-168772, 2020, doi: 10.1109/ACCESS.2020.3021212.